A novel algorithm for straightening highly curved images of human chromosome

Article *in* Pattern Recognition Letters · July 2008

DOI: 10.1016/j.patrec.2008.01.029 · Source: DBLP

2 authors:

Mehrsan Javan Roshtkhari
McGill University
23 PUBLICATIONS **342** CITATIONS
SEE PROFILE

Kamal Setarehdan
University of Tehran
93 PUBLICATIONS **712** CITATIONS
SEE PROFILE

Available online at www.sciencedirect.com
ScienceDirect
Pattern Recognition Letters 29 (2008) 1208–1217
Pattern Recognition Letters
www.elsevier.com/locate/patrec

A novel algorithm for straightening highly curved images of human chromosome

Mehrsan Javan Roshtkhari, Seyed Kamaledin Setarehdan *

Control and Intelligent Processing Center of Excellence, Faculty of Electrical and Computer Engineering, University of Tehran, Tehran, Iran

Received 10 June 2007; received in revised form 17 November 2007
Available online 15 February 2008

Communicated by T.K. Ho

Abstract

An effective chromosome image processing algorithm for straightening highly curved chromosomes is presented. This will extend the domain of application of most of the previously reported algorithms to the curved chromosomes. The proposed algorithm is based on the calculating and analyzing the vertical and horizontal projection vectors of the binary image of the chromosome obtained at various rotation angles. The binary image is obtained by thresholding the input image after histogram modification. By minimizing a rotation score S which is defined based on the relative amplitude of the main peaks in the horizontal projections of the rotated pictures, the most appropriately rotated image is identified. This picture is used to determine the *bending axis* and from which the *bending centre* of the chromosome, which is then used to artificially straighten the curved chromosome. When applied to the real images of highly curved chromosomes the proposed algorithm could straighten all of the chromosome images within the dataset. To assess the effectiveness of the proposed algorithm, the automatically extracted bending centers are compared to the manually defined ones on the whole data set. Moreover, the density profiles of the chromosomes (a one-dimensional vector obtained by intensity sampling of the chromosome along its longitudinal axis), which is the most important and most commonly used feature for classification purposes, are identified and compared before and after chromosome straightening. The quantitative analysis of the results in both cases showed a close correlation between the two.

Keywords: Curved chromosomes; Chromosome classification; Projection vectors; Chromosome straightening

1. Introduction

Many genetic disorders or possible abnormalities that may occur in the future generations can be predicted through analyzing the shape and morphological characteristics of the chromosomes. In addition to the well known genetic abnormalities like Aneuploidy (improper number of chromosomes), translocation, and deletion, some of the fatal pathological conditions like lukemia are also correlated with chromosome defects (Hong, 2000; Moradi and Setarehdan, 2006). An important standard tool to study the genetic abnormalities based on the chromosome pictures is the so called Karyotyping.

Karyotyping consists of the identification, classification and presentation of the 23 pairs of the chromosomes, obtained from a single cell either by drawing or by photography using a light microscope, in a single picture. This process, which is usually done manually by a human expert, is a difficult and time consuming task. In conventional Karyotyping, giesma banded cells are photographed under a light microscope (an example picture is shown in Fig. 1a) during the metaphase stage (one of the four stages of the cell division namely: prophase, metaphase, anaphase and telophase). In metaphase, the chromatin is condensed inside the chromosomes making them to be easily observed with a light microscope. A band is defined as part of the

* Corresponding author. Tel.: +98 21 61114177; fax: +98 21 88633029.
E-mail address: ksetareh@ut.ac.ir (S.K. Setarehdan).

0167-8655/$ - see front matter © 2008 Elsevier B.V. All rights reserved.
doi:10.1016/j.patrec.2008.01.029

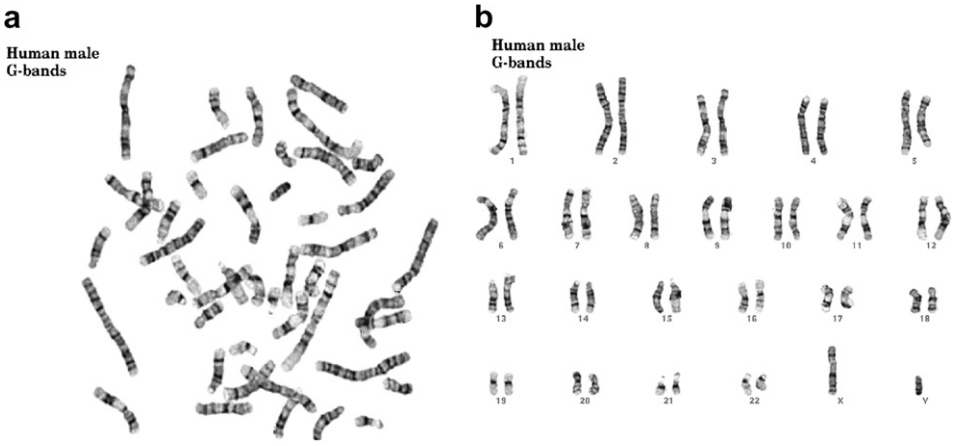

Fig. 1. (a) G-banded chromosomes of a male as seen under a microscope and (b) Karyotype developed from (a).

chromosome which is clearly distinguishable from its adjacent segments by its darker or brighter appearance. The chromosomes are visualized with a continuous series of these bright and dark bands. Each of 23 chromosomes has a specific band pattern. The result of the Karyotyping process for Fig. 1a, which is done manually by a cytogenetist is shown in Fig. 1b.

Automatic Karyotyping consists of the two main stages of segmentation and classification of the human chromosomes within the photographic pictures obtained using a light microscope. Both of the automatic chromosome segmentation and classification procedures have been a well studied problem in the last 3 decades (Moradi and Setarehdan, 2006; Castleman et al., 1976; Piper and Granum, 1989; Carothers and Piper, 1994; Agam and Dinstein, 1997; Schwartzkopf et al., 2005). Most of the classification methods, however, suffer from the natural complexity of the problem, which is caused by various unpredictable appearances of the chromosomes due to their non-rigid nature. This makes these methods to be unable to work on the curved chromosomes, although some methods could classify curved chromosomes if only the bending was less than 90° (Moradi et al., 2003).

This research has addressed the problem of automatic straightening of highly curved chromosomes after segmentation which was rarely attempted in the past (Barrett and De-Carvalho, 2003). Some commercial or research based software for image analysis provide the ability to interactively straighten curvilinear object within the image in general (Kocsis et al., 1991). Two such packages are Image/J (Rasband et al., 1997–2005) and Image SXM (Barrett and De-Carvalho, 2003). These softwares usually need the user's interaction, such as defining the two ends of the object manually. Moreover, they sometimes need the central curve of the object (e.g. chromosome) to be identified first which is a computationally expensive procedure. For example, for an image of size $n \times n$, the computation complexity for finding central curves is of order $O(n^2)$ up to $O(n^3)$ depending upon the method used for calculation (Jing and Sahni, 1992).

In this article a novel fully automatic and computationally effective algorithm for straightening the highly curved chromosomes is presented. The proposed algorithm is based on the calculation and analyzing the vertical and horizontal projection vectors of the binary image of the chromosome at different rotational angles. The binary image is obtained by thresholding the input image after histogram modification, where the appropriate threshold is automatically identified by analyzing the histogram of the image. A "*rotation score*" S is defined based on the amplitude of the main peaks in the horizontal projection vectors of the rotated pictures, which is then used to identify the most appropriately rotated image for bending axis defining. Using this picture the bending axis, hence bending centre, of the chromosome is identified, which is then used to artificially straightening the bent chromosome. The resulting straightened chromosomes can now be processed by any of the previously reported automatic chromosome classification methods.

According to the literature, most of the previously reported chromosome classification approaches use the density profile of the chromosome (a one-dimensional vector obtained by intensity sampling of the chromosome along its longitudinal axis) directly as the main feature vector (Carothers and Piper, 1994). Some other methods use a reduced version of the density profile or a set of the second class features obtained from the density profile (Moradi and Setarehdan, 2006; Piper and Granum, 1989; Guimaraes et al., 2003,; Nanni, 2006). In (Lerner et al., 1995) a reduced version of the density profile is developed and used based on such sub-optimal methods as the knockout method. In (Qiang and Castleman, 2000) the features extracted from the weighted density distribution and in (Sweeney et al., 1997) the Fourier transformation or the Wavelet transformations of the density profile were used.

Due to the importance of the density profile as the most important and commonly used chromosome feature vector, in this paper we used the density profile to evaluate the effectiveness of the proposed algorithm. For this purpose, we quantitatively compared the density profiles of the

straightened chromosomes to that of the original chromosomes where the latter was defined manually.

The rest of the paper is organized as follows: Section 2 introduces the chromosome image data set used in this study. In Section 3, the block diagram of the proposed algorithm together with the function of each block is explained. The results of the application of the proposed algorithm and assessment procedure to the real chromosome images are presented in Section 4. Finally Section 5 concludes the paper.

2. The dataset

The chromosome images used in this study include images of chromosomes number 16, 17 and 18 which are taken from the data set that we developed and used in one of our previously reported research works (Moradi and Setarehdan, 2006). They were produced in the Cytogenetic Laboratory of Cancer Institute, Imam Hospital, Tehran, Iran. The images were acquired by a conventional photography system using a light microscope (Leitz, ortholux) with a magnification factor of 100X. The chromosomes were segmented from the pictures by an expert in the Cytogenetic Laboratory and then scanned by a scanner (Microtek, ScanPlus6) with a resolution of 300 dpi. The gray scale resolution of the resulting digitized pictures was set to 256 levels. The dataset includes 303 curved chromosome pictures mostly of size 120×80 pixels obtained from 76 different patients (three pairs of chromosomes from 25 patients and three single chromosomes from 51 patients).

Due to the various amounts of the bend angles of the curved chromosomes in the data set, Table 1 shows the distribution of the bend angles over a range defined as the "Extremely curved", "Highly curved", "Curved", and "Slightly curved" chromosomes as defined in Table 1. As seen from Table 1, almost 80% of the chromosomes are highly curved or extremely curved. The image data set is randomly divided into the training and test sets each of 193 and 110 images, respectively. Due to the relatively small number of the available data samples and for a more valid generalization, the randomly dividing of the dataset into the training and test sets was carried out 20 times. The training sets will be used to determine the appropriate values of the tuning parameters of the algorithm in Section 3.3 while the test sets will be used to evaluate the complete proposed algorithm in Section 4. The resulting values of the 20 experiments will then be averaged to determine the final results in each case.

3. Proposed algorithm

The block diagram of the proposed algorithm for straightening highly curved chromosomes is shown in Fig. 2. In continue each block will be explained in more details.

3.1. Binary image production

The strategy in the proposed chromosome straightening algorithm is to define the bending axis, hence bending centre, of the curved chromosome first. The bending centre of a curved chromosome is a morphological feature which can be easier identified in the binary image of the chromosome than the original gray scale image. Therefore, it is a necessary step to produce the binary image of the chromosome first.

A chromosome image can be considered as a bimodal image (Vernon, 1991), in which an object (chromosome) is lying on a uni-color background with a different gray

Table 1
The distribution of the bend angles of the chromosomes in the dataset

	Extremely curved (more than 140°)	Highly curved (between 90° and 140°)	Curved (between 60° and 90°)	Slightly curved (less than 60°)
Chromosomes in the dataset (%)	22.8	56.4	11.9	8.9

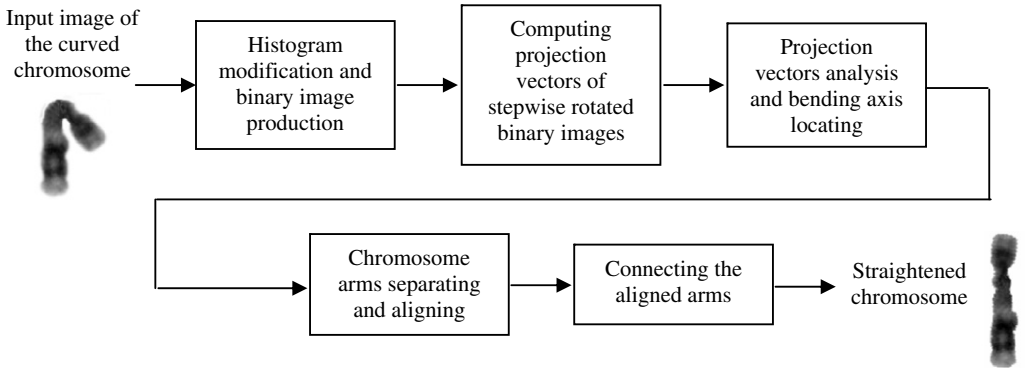

Fig. 2. Block diagram of the proposed automatic chromosome straightening algorithm.

scale value. Histogram of such an image usually includes two peaks, one of which corresponds to the background pixels and the other corresponds to the object pixels. An effective threshold value to separate the object from the background in a bimodal image can be determined by locating the global minimum of the histogram residing between the two above mentioned maxima (Moradi et al., 2003). The gray value representing the global minimum is the appropriate threshold value. Using this threshold all those pixels with a gray value smaller than the threshold are set to 1 (white) and the remaining pixels are set to 0 (black) producing the binary format of the input image. An example chromosome image, its histogram and the binary version of the chromosome are shown in Fig. 3a–c, respectively.

3.2. Computing projection vectors of stepwise rotated binary image

Theoretically, the two orthogonal projection vectors (horizontal and vertical) of the binary image of the chromosome contain all the morphological information of the object and can be used for binary image reconstruction and/or for feature extraction. For example they can be used to calculate the extent of the chromosome (i.e. where the chromosome begins and ends on the image plane), locating the centromere of the chromosome (the narrowest part of the chromosome which divides it into the short and long arms) (Moradi and Setarehdan, 2006), or as it will be shown shortly, they can be used for locating the bending centre of the curved chromosomes.

In order to calculate the horizontal projection vector, simply the pixel values of each row are summed up in the binary image. Considering that the binary image includes only 1s (white pixels) and 0s (dark pixels), therefore, each element of the horizontal projection vector is equal to the number of white pixels (1s) in the corresponding row. Fig. 4 demonstrates a binary image of a sample chromosome number 16 and its horizontal projection vector.

As seen, in the case of this straight chromosome the global minimum occurring in between the two locally global maxima in the central part of the projection vector corresponds to the centromere of the chromosome, where the chromosome has the least width. Finding the two maxima

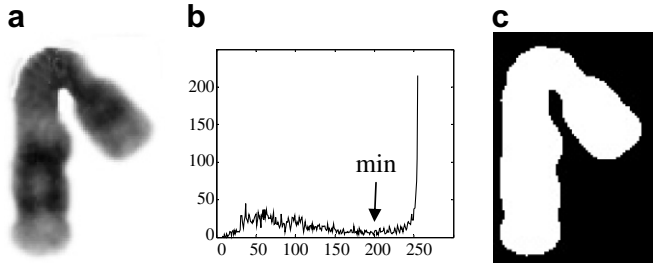

Fig. 3. (a) An example highly curved chromosome from the data set, (b) the histogram of the chromosome in (a) and (c) its binary version.

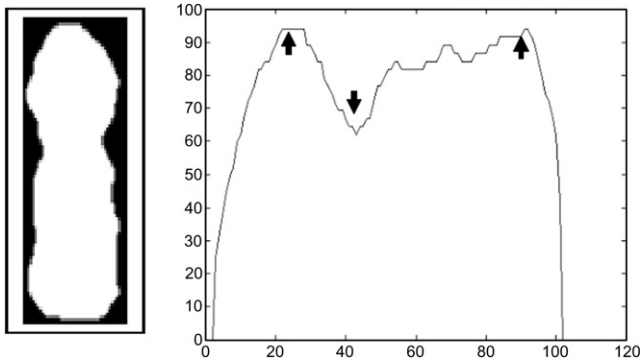

Fig. 4. A binary image of a sample chromosome number 16 and its horizontal projection vector. The main two locally global maxima and the global minimum point in between them are marked over the plot.

and the global minimum points on the horizontal projection vector and mapping them on to the chromosome picture, an automatic centromere locating algorithm was developed and published in one of our past works (Moradi et al., 2003, 2006).

A similar idea for locating the bending centre of the curved chromosomes is developed in the current article. For a highly curved chromosome (90° or more), however, the projection vector has no a simple description. Depending upon the position of the curved chromosome within the image and the degree of bending a different plot for the horizontal projection vector will be obtained, which may have one or more locally global maxima points with different relative heights. For this reason, the idea of stepwise rotating the binary chromosome image and analyzing their corresponding horizontal projection vectors was developed in this paper.

3.3. Projection vectors analyzing and bending centre locating

At this stage, the horizontal projection vectors of the stepwise rotated highly curved chromosome pictures are calculated and analyzed. For any rotation step of 10°, starting from 0° up to the 180°, the horizontal projection vectors are calculated. As mentioned before, depending upon the position of the curved chromosome within each rotated image, there might be one or more locally global maxima with various amplitudes in the corresponding projection vector. Fig. 5 shows the horizontal projection vectors obtained for a sample highly curved chromosome image rotated from 0° to 180° in 10° steps.

By inspecting the set of the rotated images and corresponding projection vectors it can be seen that for any rotated image whose projection vector includes two locally global maxima points with their amplitudes almost equal, the global minimum point in between them corresponds to the bending centre of the curved chromosome. As with the example chromosome of Fig. 5 this may happen in more than one rotation steps. As seen in Fig. 5, this situation has happened in four rotation steps from 50° to 80°. However, by comparing these four cases, it can be

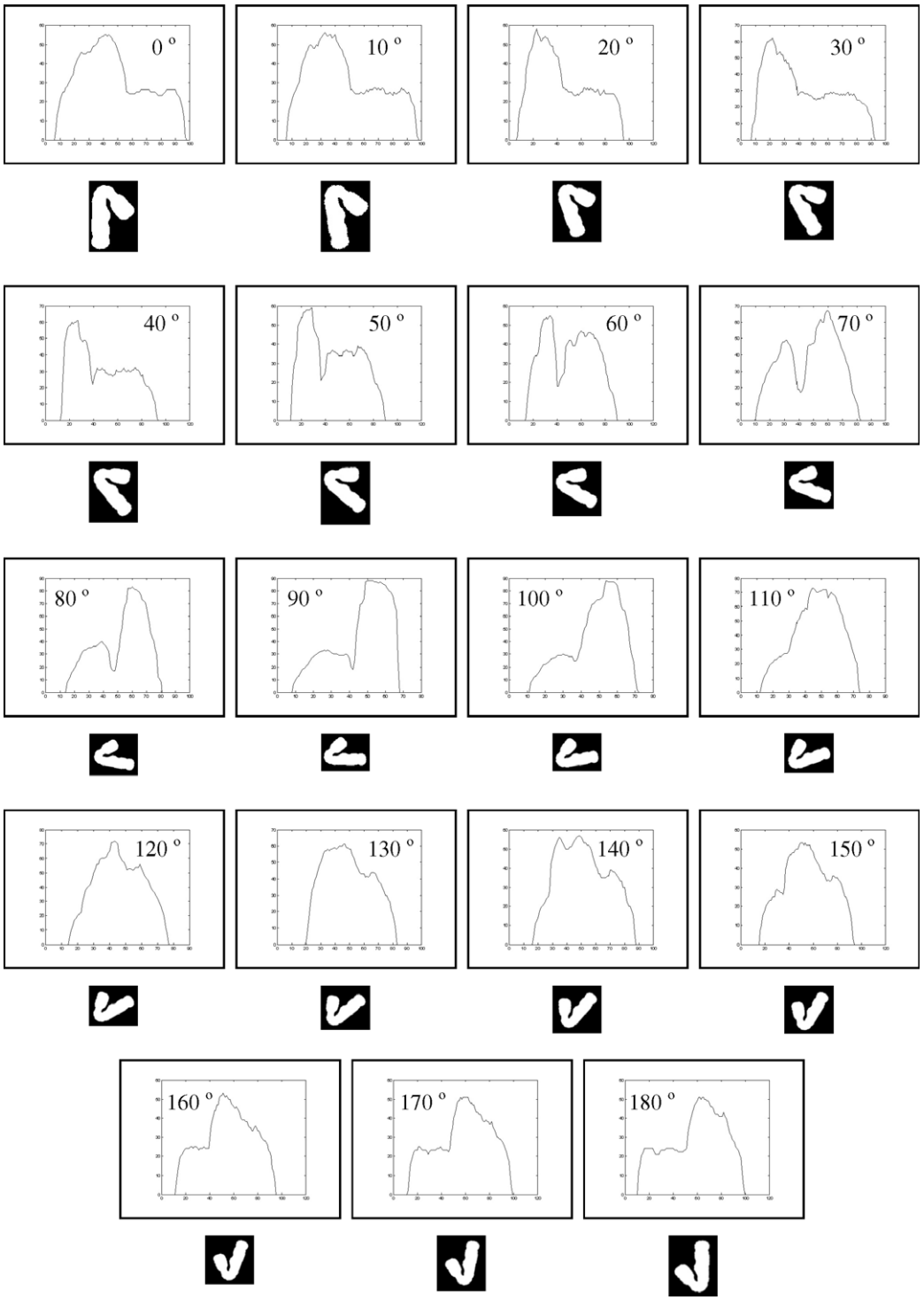

Fig. 5. The horizontal projection vectors obtained for a sample highly curved chromosome image rotated from 0° to 180° in 10° steps.

concluded that the image with the comparatively smallest global minimum residing in between the two comparatively largest maxima points (with almost equal amplitudes) is the target image (the image with the rotation angle of 60° in this example).

Based on this and other similar observations and in order to automatically identify the target image, a rotation score S is defined as follows:

$$S = w_1 \times R_1 + w_2 \times R_2 \tag{1}$$

where

$$R_1 = |P_1 - P_2|/(P_1 + P_2) \tag{2}$$

and

$$R_2 = P_3/(P_1 + P_2) \tag{3}$$

In Eqs. (2) and (3), P_1 is the magnitude of the largest locally global maximum, P_2 is the magnitude of the second locally global maximum and P_3 is the magnitude of the global minimum residing in between the two. Eq. (2) describes that if the two locally global maxima have almost equal amplitudes, then case R_1 will have a smaller value. R_2 describes the relative amplitude of the global minimum in between the two locally global maxima points. Of course, the target rotated image is the one for which the rotation score S is minimum. The global minimum in the horizontal projection vector of such image corresponds to the bending centre of the chromosome.

The coefficients w_1 and w_2 in Eq. (1) are the tuning parameters to control the weight of each term in the rotation score S where $w_1 < 1$, $w_2 < 1$ and $w_1 + w_2 = 1$. An extensive iterative search procedure was carried out to determine the appropriate values of the tuning parameters w_1 and w_2 for the data set in hand. For all values of the tuning parameters within their possible variation range ($w_1 < 1$, $w_2 < 1$ and $w_1 + w_2 = 1$) and in steps of 0.01 the bending axis, hence bending centre, is determined for all of the images within each training set by the proposed automatic algorithm. These are compared to the bending centers which are identified manually. The root mean squared of the difference between the two are then minimized over the whole possible values of the tuning parameters. The tuning parameters are calculated in this way for all 20 training sets. The final values of the tuning parameters are then defined by averaging the resulting 20 values for each parameter. Table 2 demonstrates the final values and the statistical distribution of the tuning parameters w_1 and w_2.

Using the values obtained for parameters w_1 and w_2 as described earlier, the S values for the rotated pictures of Fig. 5 are calculated and shown in Table 3. As seen, the image rotated by 60° has showed the smallest S value hence this is the target image. The location of the extracted global minimum in the horizontal projection vector of this image corresponds to the bending centre. The horizontal line passing through the point on the chromosome image coincident with the global minimum point in the horizontal projection vector represents the bending axis of the chromosome as shown in Fig. 6 for the example target image. The most outward intersecting point between the bending axis and the chromosome body, as marked with a circle in Fig. 6, is the so called *bending centre* of the curved chromosome.

One last point to end this section is that as described before it is necessary to locate the two locally global maxima and the global minimum point in between them within the projection signals. The accuracy of this procedure can be affected by the small local maxima and minima points in any projection signal. To solve this problem, signal smoothing is necessary prior or simultaneous to maxima and minima locating process. In this work, the fuzzy multi-resolution based signal processing algorithm for singular point (edge or peak) locating in a very noisy signal of Setarehdan (1998), Setarehdan and Soraghan (1999) is employed. Using the Mallat's non-orthogonal wavelet transform (Mallat and Zhong, 1992) and the second derivative of the Gaussian function as the mother wavelet it is shown that the wavelet transform is equivalent to a peak detector operator. Using the non-orthogonal wavelet transform of Mallat, the method developed in (Setarehdan, 1998; Setarehdan and Soraghan, 1999) combines the peak information in the wavelet transform scales in a novel fuzzy manner to come up with a very robust peak (maximum or minimum point) locating algorithm.

Table 2
Final values and the statistical distribution of the tuning parameters w_1 and w_2 obtained over 20 experiments

	Minimum value	Maximum value	Mean	Standard deviation
w_1	0.42	0.46	0.434	0.031
w_2	0.54	0.58	0.566	0.028

Table 3
The S values obtained for the rotated images of Fig. 5

Rotation score S	Rotation (°)
0.4425	0
0.4691	10
0.4592	20
0.4618	30
0.4664	40
0.3501	50
0.2398	**60**
0.2498	70
0.3213	80
0.4524	90
1.5043	100
1.2139	110
1.2274	120
1.1904	130
1.1212	140
0.9541	150
0.5211	160
0.4695	170
0.4426	180

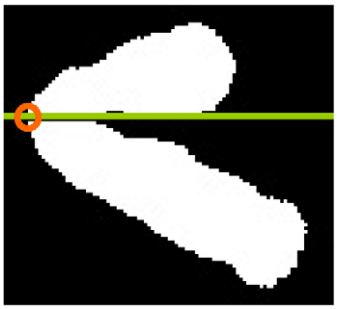

Fig. 6. The target binary image (60° rotated image in the example of Fig. 5) together with its bending centre and bending axis automatically identified.

3.4. Chromosome arms alignment procedure

Locating the bending axis and bending centre of the chromosome, the image can now be easily straightened as

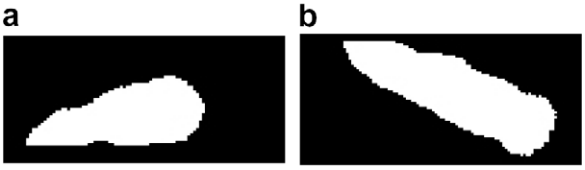

Fig. 7. (a) The upper arm and (b) the lower arm of the chromosome in Fig. 6.

explained next. The binary image is first separated into two sub-images along the bending axis as shown in Fig. 7 for the example chromosome in Fig. 6. Each sub-image contains one arm of the chromosome which is approximately a straight object. The two sub-images must now be rotated so that the two arms to be in the same direction, for example both be vertical. For this purpose, each sub-image is rotated while its vertical projection vector is calculated at each rotation step. Due to the particular shape of each arm of the chromosome, the vertical projection vector will demonstrate minimum width if the arms to be in the vertical position inside the sub-image. This is shown for the lower arm of Fig. 7 in Fig. 8.

Table 4 demonstrates the width of the vertical projection vector computed for various rotation angles of the lower arm. As seen in Fig. 8 and in Table 4, the image of the lower arm rotated by 60° is in the vertical position and in the same time presents minimum width in the vertical projection vector.

In a similar manner, the upper arm is rotated so to be in the vertical position. Now we are in the position to apply the same procedure to the real gray scale image rather than its binary version. Fig. 9a shows the corresponding gray scale image of the binary chromosome with the bending axis and bending centre superimposed, while Fig. 9b demonstrates its two arms after aligning in the vertical direction.

Table 4
The number of non-zero elements (width) of the vertical projection vectors shown in Fig. 8

Number of non-zero elements (width) of the vertical projections	Rotation (°)
82	0
75	10
66	20
57	30
47	40
36	50
26	**60**
30	70
37	80
47	90

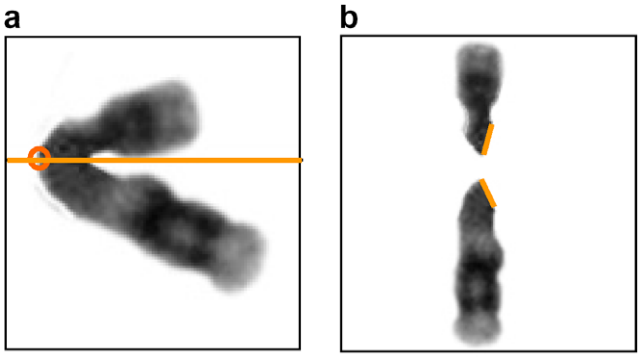

Fig. 9. (a) The original gray scale image with the automatically identified bending axis and the bending centre overlaid and (b) the two chromosome arms after separating and aligning in the vertical direction.

Next, the two aligned gray scale images of the chromosome arms must be connected to produce the final straightened chromosome picture (Fig. 10).

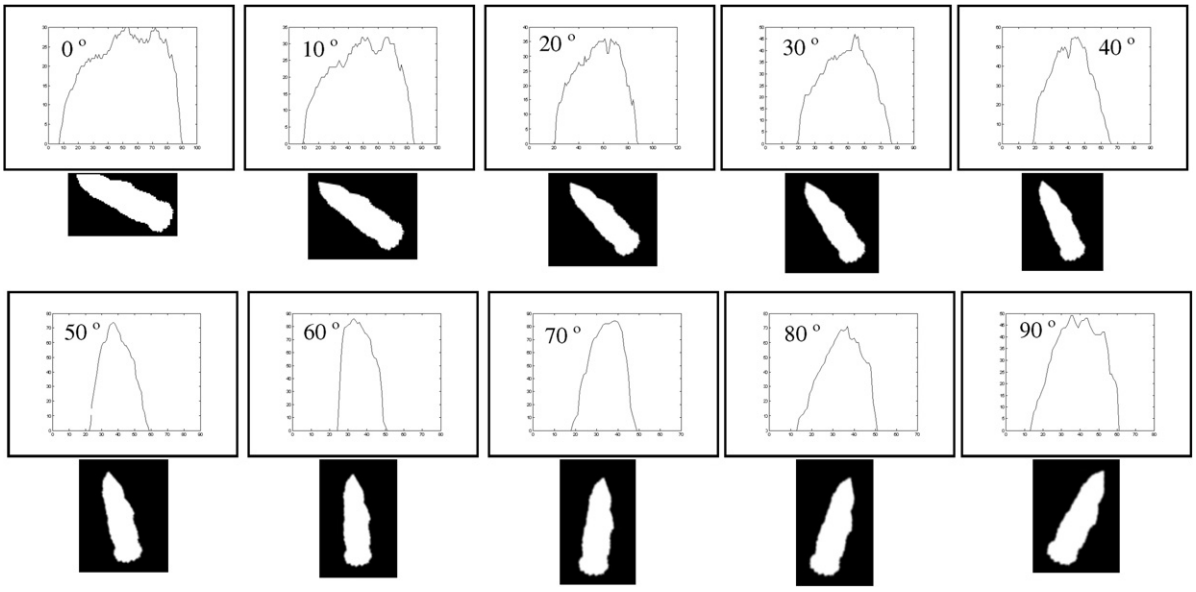

Fig. 8. The vertical projection vectors obtained for the lower arm of the example chromosome in Fig. 7b.

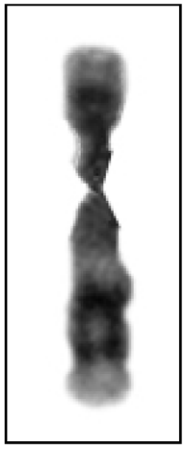

Fig. 10. The final straightened chromosome.

4. Evaluation of the proposed algorithm

Evaluation of the proposed automatic chromosome straightening algorithm is comprised of three sections as explained in follows.

4.1. Evaluation of the bending center locating procedure

First, the bending centre locating procedure of Section 3.3 is evaluated by applying it to each test set. The reference bending centers are also manually identified for comparison purposes. The comparison is carried out and presented in Table 5 in terms of the *mean* and *standard deviation* and *maximum* values of the Euclidean distances between the two, obtained over the entire test sets. For a more meaningful comparison, each distance value is also normalized with the length of the chromosome and the three parameters of *mean*, *standard deviation* and *maximum* values are calculated again and shown in Table 5. For this purpose, the length of the chromosomes is also determined manually. As seen in Table 5, the absolute and normalized errors are very small.

4.2. Evaluation of the alignment procedure

For evaluating the performance of the alignment procedure of Section 3.4, the bend angles of the curved chromosomes within the test data set are calculated manually, which is then compared to the sum of the rotation degrees of the two arms of the chromosomes subtracted from 180°. Table 6 presents the comparative results in terms of the *mean*, the *standard deviation* and the *maximum* values of the differences between the two, obtained over the test sets of all 20 experiments. Considering that the rotating steps of the chromosome arms in the alignment procedure was 10°, the comparative results of Table 6 are quite satisfactory.

Table 5
Difference between the automatically defined bending centers to manually defined ones

Absolute distance	
Mean (pixels)	2.48
Standard deviation (pixels)	1.72
Maximum (pixels)	3
Normalized distance	
Mean	0.0184
Standard deviation	0.013
Maximum	0.023

Table 6
The quantitative study of the accuracy of the alignment procedure (for more information see the text)

Mean (°)	7.3
Standard deviation (°)	4.6
Maximum (°)	11.4

4.3. Evaluation of the proposed algorithm using the density profiles

For evaluating the proposed algorithm as a whole, next the density profiles of the original and straightened chromosomes are extracted and compared to each other. As mentioned before, most of the chromosome classification approaches use the density profile of the chromosome directly or indirectly as the main feature vector (Moradi and Setarehdan, 2006; Piper and Granum, 1989; Nanni, 2006; Lerner et al., 1995; Qiang and Castleman, 2000). Therefore, having in mind that the automatic chromosome classification is the ultimate goal of the chromosome

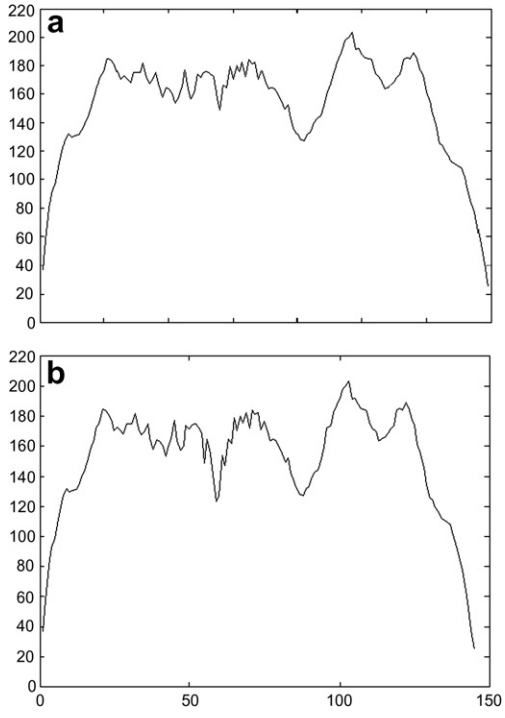

Fig. 11. Comparison of the density profiles for the chromosomes in Figs. 3a (top) and 10b (bottom), respectively.

Table 7
Root mean squared differences (RMSD) between the two corresponding intensity profiles of the chromosomes before and after straightening procedure

Mean	0.0386
Standard deviation	0.00367
Maximum	0.0407

straightening procedure and also the fact that the chromosome intensity profile is the most important feature vector for this purpose, we have compared the intensity profiles of the chromosomes in the data set before and after chromosome straightening. For extraction of the density profiles the longitudinal axis of the chromosomes are defined manually before and after straightening. Then each sample of the density profile is defined as the average intensity of the pixels lying on a line perpendicular to the longitudinal axis of the chromosome as explained in (Moradi and Setarehdan, 2006). Fig. 11a and b shows the intensity profiles of the example chromosome of Figs. 3(a) and 10(b), respectively. As seen, there is a very small visually recognizable difference between the two.

For a quantitative analysis, the comparison is carried out on all chromosome images within the 20 test sets in terms of the root mean squared differences (RMSD) between the two corresponding intensity profiles. The *mean*, *standard deviation* and *maximum* of the RMSDs were calculated and shown in Table 7.

As it can be seen from Table 7, the comparative study shows a close correlation between the chromosome density profiles before and after straightening which is the main feature used for chromosome identification and classification in most automatic algorithms.

5. Conclusion

In this paper, a simple yet effective chromosome image processing algorithm for straightening highly curved chromosomes was presented. The proposed algorithm is based on the calculation and analyzing the vertical and horizontal projection vectors of the binary image of the chromosome obtained at various rotation angles. A *rotation score S* was defined based on the relative amplitude of the main peaks in the horizontal projection vectors of the rotated pictures. The most appropriately rotated image was then identified by minimizing the S value over the rotation angle. This image was used next to determine the bending axis and bending centre of the chromosome. The chromosome was then separated into its two arms along the bending axis. The arms are then aligned and reconnected to produce the final straightened chromosome.

For evaluation of the proposed algorithm it was applied to the real images of the curved chromosomes with various degrees of the bend angles within the data set (with 80% of them being highly or extremely curved as explained in Table 1). The data set was randomly divided into the training and test sets each of 193 and 110 images, respectively. Due to the relatively small number of the available data samples and for a more valid generalization, the randomly dividing of the dataset into the training and test sets was repeated 20 times and the results were averaged. The training sets were used to determine the appropriate values of the tuning parameters of the algorithm while the test sets were used to evaluate the performance of the proposed algorithm.

Three evaluation procedures were carried out in this work including evaluation of the bending centre locating procedure, evaluation of the alignment procedure, and evaluation of the proposed algorithm as a whole by quantitative comparison of the density profiles of the chromosomes (a one-dimensional vector obtained by intensity sampling of the chromosome along its longitudinal axis) which were manually obtained before and after straightening procedure.

The quantitative comparative study showed a close correlation between the density profiles (before and after straightening) in terms of the root mean squared differences (RMSD) between the two corresponding intensity profiles averaged over the entire number of the test data samples in 20 experiments (Table 7).

Since the intensity profile is one of the main features used for chromosome identification and classification in most previously reported automatic algorithms, therefore, the proposed algorithm extends the domain of the application of most of the previously published algorithms to the highly curved chromosomes.

It should be noted that the proposed chromosome straightening algorithm uses only the morphological features of the binary image of the chromosomes, which is not severely affected by the quality of the imaging system. Therefore, it can be concluded that the algorithm is independent of the dataset.

As a final point, although the proposed chromosome straightening algorithm performs quiet well on the chromosomes in group E (chromosomes 16–18), however, it is not expected to perform always as well on some other chromosomes like chromosomes in Group A and B, which are long and in some cases may have more than one bending centers. In other words, as the proposed algorithm assumes a single "bend center" and straight arms, these requirements may not be always satisfied by the chromosomes in some other classes. As a further research step of current work, the performance of the proposed algorithm on other classes of chromosomes needs to be studied. This of course needs to develop a complete data set with an appropriately large number of bent chromosomes from other classes, which is currently under progress by the authors.

References

Agam, G., Dinstein, I., 1997. Geometric separation of partially overlapping nonrigid objects applied to automatic chromosome classification. IEEE Trans. Pattern Anal. Mach. Intell. 19, 1212–1222.

Barrett, S.D., De-Carvalho, C.R., 2003. A software tool to straighten curved chromosome images. J. Chromosome Res. 11, 83–88.

Carothers, A., Piper, J., 1994. Computer-aided classification of human chromosomes: A review. Statist. Comput. 4, 161–171.

Castleman, K.R., Melnyk, J.H., 1976. Automated System for Chromosome Analysis, Final Report, JPL Document No. 5040-30, Jet Propulsion Laboratory, Pasadena, California.

Guimaraes, L.V., Schuck, A., Elbern, A., 2003. Chromosome classification for karyotype composing applying shape representation on Wavelet packet transform. In: Proc. 25th Annual Internat. Conf. of the IEEE EMBS, pp. 941–943.

Hong, L.M., 2000. Medical Cytogenetics, first ed. Marcel Dekker, New York.

Jing, F.J., Sahni, S., 1992. Serial and parallel algorithms for the medial axis transformation. IEEE Trans. Pattern Anal. Mach. Intell. 14, 1218–1224.

Kocsis, E., Trus, B.L., Steer, C.J., Bisher, M.E., Steven, A.C., 1991. Image averaging of flexible fibrous macromolecules: The clathrin triskelion has an elastic proximal segment. J. Struct. Biol. 107, 6–14.

Lerner, B., Guterman, H., Dinstein, I., Romem, Y., 1995. Medial axis transform-based features and a neural network for human chromosome classification. Pattern Recognition 28, 1673–1683.

Mallat, S., Zhong, S., 1992. Characterization of signals from multiscale edges. IEEE Trans. Pattern Anal. Mach. Intell. 14, 710–732.

Moradi, M., Setarehdan, S.K., 2006. New features for automatic classification of human chromosomes: A feasibility study. Pattern Recognition Lett. 27, 19–28.

Moradi, M., Setarehdan, S.K., Ghaffari, S.R., 2003. Automatic landmark detection on chromosomes images for feature extraction purposes. In: Proc. 3rd Internat. Symp. on Image and Signal Processing and Analysis (ISPA), pp. 567–570.

Moradi, M., Setarehdan, S.K., Ghaffari, S.R., 2003. Automatic locating the centromere on human chromosome pictures. In: Computer-based Medical Systems, pp. 56–61.

Nanni, L., 2006. A reliable method for designing an automatic karyotyping system. J. Neurocomput. 69, 1739–1742.

Piper, J., Granum, E., 1989. On fully automatic feature measurement for banded chromosome classification. Cytometry 10, 242–255.

Qiang, W., Castleman, K.R., 2000. Automated chromosome classifier using wavelet-based descriptors. In: Proc. IEEE Symp. on Computer Based Medical Systems, pp. 189–194.

Rasband, W.S., 1997–2005. Image J, National Institutes of Health, Bethesda, Maryland, USA. <http://rsb.info.nih.gov/ij>.

Schwartzkopf, W.C., Bovik, A.C., Evans, B.L., 2005. Maximum-likelihood techniques for Joint segmentation-classification of multispectral chromosome images. IEEE Trans. Med. Imag. 24, 1593–1610.

Setarehdan, S.K., 1998. Echocardiographical Cardiac Function Assessment and Wall Motion Visualisation using Fuzzy Logic and the Wavelet Transform. PhD Thesis, University of Strathclyde, February.

Setarehdan, S.K., Soraghan, J.J., 1999. Fuzzy multiresolution signal processing. In: Proc. 3rd World Multiconference on Systemics, Cybernetics and Informatics (SCI'99) and 5th Internat. Conf. on Information Systems Analysis and Synthesis (ISAS'99), Orlando, USA.

Sweeney, N., Becker, R.L., Sweeney, B., 1997. A comparison of wavelet and Fourier descriptors for a neural network chromosome classifier. In: 19th IEEE EMBS Conf., pp. 1359–1362.

Vernon, D., 1991. Machine Vision, first ed. Prentice-Hall, UK.